JACS
JOURNAL OF THE AMERICAN CHEMICAL SOCIETY
Article
pubs.acs.org/JACS

Origins of Regioselectivity in Iridium Catalyzed Allylic Substitution

Sherzod T. Madrahimov,[‡] Qian Li,[§] Ankit Sharma,[§] and John F. Hartwig*[,‡,§]

[‡]Department of Chemistry, University of Illinois, 600 South Mathews, Urbana, Illinois 61801, United States
[§]Department of Chemistry, University of California, Berkeley, California 94708, United States

Supporting Information

ABSTRACT: Detailed studies on the origin of the regioselectivity for formation of branched products over linear products have been conducted with complexes containing the achiral triphenylphosphite ligand. The combination of iridium and $P(OPh)_3$ was the first catalytic system shown to give high regioselectivity for the branched product with iridium and among the most selective for forming branched products among any combination of metal and ligand. We have shown the active catalyst to be generated from $[Ir(COD)Cl]_2$ and $P(OPh)_3$ by cyclometalation of the phenyl group on the ligand and have shown such species to be the resting state of the catalyst. A series of allyliridium complexes ligated by the resulting P,C ligand have been generated and shown to be competent intermediates in the catalytic system. We have assessed the potential impact of charge, metal−iridium bond length, and stability of terminal vs internal alkenes generated by attack at the branched and terminal positions of the allyl ligand, respectively. These factors do not distinguish the regioselectivity for attack on allyliridium complexes from that for attack on allylpalladium complexes. Instead, detailed computational studies suggest that a series of weak, attractive, noncovalent interactions, including interactions of H-bond acceptors with a vinyl C—H bond of the alkene ligand, favor formation of the branched product with the iridium catalyst. This conclusion underscores the importance of considering attractive interactions, as well as repulsive steric interactions, when seeking to rationalize selectivities.

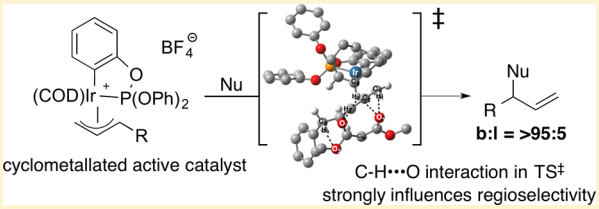

INTRODUCTION

Allylic substitutions catalyzed by cyclometalated iridium phosphoramidite complexes[1−4] have become processes studied by many researchers[5−13] and used in synthetic applications.[14] Such cyclometalated systems catalyze allylic substitution reactions with high selectivity for the formation of branched allylic substitution products.[3,4] Mechanistic studies on reactions catalyzed by these iridium complexes have revealed the resting state of the catalyst, the origins of enantioselection, and the importance of cyclometalation to generate the active catalyst.[15−18] However, mechanistic studies of reactions catalyzed by iridium complexes of triphenylphosphite, the first system shown by Takeuchi to give branched products from linear allylic carbonates[19−21] are limited. A cyclometalated species was proposed to be the active catalyst, but this species was never observed directly and characterized.[22] Most importantly, the origin of the high selectivity for the formation of the branched product has not been revealed for reactions catalyzed by complexes of either phosphite or phosphoramidite ligands.

Palladium catalyzed allylic substitution reactions typically give products from allylic substitution in which the nucleophile adds to the least hindered terminus.[23,24] Thus, palladium-catalyzed allylic substitution with monosubstituted allylic electrophiles give linear allylic substitution products. Many theories have been proposed to account for the regioselectivity of allylic substitution reactions.[24,25] These theories include reaction at the terminus with the longer metal−carbon bond,[26] reaction at the site with the greater positive charge,[27] reaction trans to the softer donor of a ligand with phosphorus and nitrogen donors,[26,28−34] reaction at the alkyl terminus of an eneyl structure,[35] and reaction to form the more stable metal-alkene complex as product.[36,37] In addition, studies have shown that the isomer formed as product can be derived from a thermodynamic selectivity, rather than a kinetic selectivity. For example, Yudin and co-workers showed that the branched substitution product was kinetically favored for reactions of amines with an allylpalladium species, but the initially formed branched product isomerized to the thermodynamically more stable linear product during the course of the reaction.[38,39]

Here we describe the preparation of Ir(I) and Ir(III) complexes containing cyclometalated triphenylphosphite ligands and detailed studies to provide insight into the origin of the high regioselectivity for formation of the branched product from iridium-catalyzed allylic substitutions. The kinetic competence of the corresponding allyliridium complexes to be intermediates in allylic substitution reactions catalyzed by iridium-triphenylphosphite complexes was confirmed by their reactions with stabilized carbon and heteroatom nucleophiles. The isolated Ir(I) and Ir(III) complexes then serve as a tool to reveal the origins of regioselectivity of iridium-catalyzed allylic substitution reactions. The ligands trans to the two allyl termini are distinct and fortuitously lead to nearly identical Ir—C distances to the two allyl termini. A combination of experimental studies with these complexes and detailed computation show that the major factor favoring the formation of the branched product is not the

Received: August 22, 2015
Published: October 26, 2015

DOI: 10.1021/jacs.5b08911
J. Am. Chem. Soc. 2015, 137, 14968−14981

presence of the phosphorus ligand trans to the substituted allylic terminus, the metal−carbon bond distance, or the relative binding affinities of terminal olefins over branched olefins to the different metal centers. Instead, the computational data suggest that a series of weak, attractive, noncovalent interactions, including interactions of H-bond acceptors with a vinyl C—H bond of the alkene ligand, favor formation of the branched product with the iridium catalyst.

RESULTS AND DISCUSSION

Preparation and Characterization of Complexes of Iridium and Palladium. To reveal the differences in the regioselectivity of allylic substitution reactions catalyzed by iridium and palladium complexes, we prepared monosubstituted allyliridium complexes of the achiral triphenylphosphite ligand and monosubstituted allylpalladium complexes of the achiral DPPF ligand. As will be seen from their structures, these two types of complexes allowed us to assess the importance of the donor group trans to the two ends of the allyl unit and the relative metal−carbon bond lengths in the ground-state structure on the regioselectivity for attack of the nuclei on the two termini of the allyl group.

Preparation of Ir(III) and Ir(I) Complexes Containing Cyclometalated Triphenylphosphite Ligand. Allyliridium complexes containing a cyclometalated triphenylphosphite ligand formed from the reaction of $[Ir(COD)Cl]_2$, triphenylphosphite, $AgBF_4$ and an allylic carbonate (Scheme 1). This

Scheme 1. Preparation of Allyliridium Complexes 3a and 3b

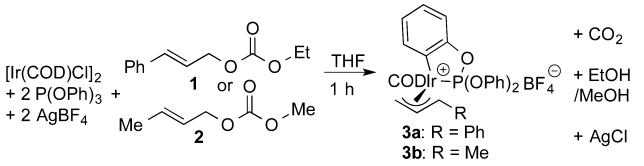

reaction is similar to that reported by Helmchen and co-workers for the preparation of allyliridium complexes containing cyclometalated phosphoramidite ligands.[40] To prepare the allyl complexes containing an iridacycle derived from triphenylphosphite, $[Ir(COD)Cl]_2$ was combined with $P(OPh)_3$ in THF to form $P(OPh)_3Ir(COD)Cl$. A solution of $AgBF_4$ in THF was added to the solution of $[P(OPh)_3]Ir(COD)Cl$, followed by an allylic carbonate. Allyliridium complexes **3a** and **3b** were formed in 1 h and were isolated in 80% and 85% yields, respectively. Carbon dioxide, ethanol, or methanol and AgCl were the byproducts of this reaction.

Preparation of Ir(I) complexes containing a single cyclometalated triphenylphosphite ligand proved to be more challenging than the preparation of allyliridium(III) complexes containing this ligand. Initially we attempted to prepare Ir(I) complexes by base-assisted cyclometalation of coordinated triphenylphosphite, followed by trapping of the formed cyclometalated complex with an alkene ligand, as we reported for complexes of cyclometalated phosphoramidite ligands.[16] However, the reaction shown in Scheme 2a formed an iridium(III) hydride ligated by two cyclometalated phosphites and one κ^1-phosphite, as evidenced by three doublets of doublets in the ^{31}P NMR spectrum, and a doublet of triplets at −8.9 ppm in the ^1H NMR spectrum. The same complex formed quantitatively from the reaction of $[Ir(COD)Cl]_2$ with 6 equiv of triphenylphosphite in the presence of an amine base (Scheme 2b).

Scheme 2. Attempts to Prepare Cyclometalated Ir(I) Complex through Base Assisted Cyclometalation

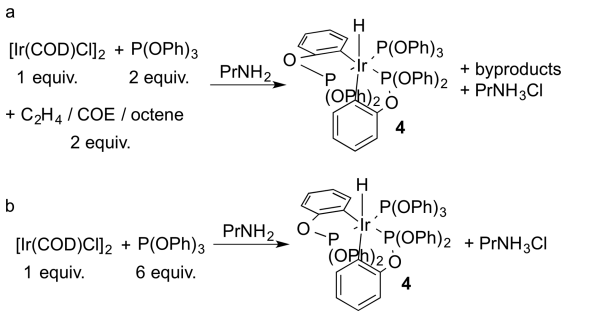

Instead, Ir(I) complex containing a single cyclometalated triphenylphosphite **5** was prepared bynucleophilic attack on cinnamyl or crotyl iridium complexes **3a** or **3b** containing cyclometalated triphenylphosphite. Complex **3b** was chosen as the most suitable allyliridium complex for this procedure because the addition of propylamine would form a volatile allylic amine product. According to this procedure, crotyliridium complex **3b** was treated with an excess of propylamine. After nucleophilic attack, the reaction vessel was exposed to 1 atm of ethylene to form the ethylene-ligated complex **5** in 85% isolated yield (Scheme 3).

Scheme 3. Preparation of the Ethylene-Ligated Cyclometalated Ir(I) Complex by Nucleophilic Attack on Allyliridium Complex 3b, Followed by a Ligand Exchange

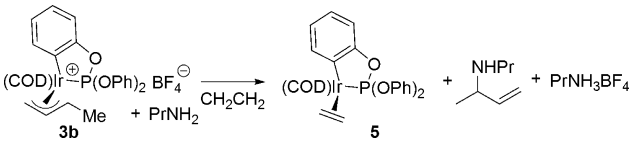

Characterization of the Cyclometalated Ir(III), Ir(I) Complexes. Cinnamyliridium complex **3a** and crotyliridium complex **3b** containing iridacyclic centers both form as a mixture of two diastereomers, as determined by ^{31}P NMR spectroscopy. The ^{31}P NMR spectra of the two diastereomers of cinnamyl complex **3a** in CH_2Cl_2 consisted of resonances at 97.0 and 95.7 ppm in a 70:30 ratio, respectively. The ^{31}P NMR spectra of the two diastereomers of crotyliridium complex **3b** formed in CH_2Cl_2 consisted of resonances at 99.4 and 97.1 ppm in a 43:57 ratio. Both complexes are sparingly soluble in THF. Single crystals were obtained of **3a** that were suitable for X-ray crystallographic analysis.

Bulk crystalline samples of both cinnamyl and crotyl complexes **3a** and **3b** consist of one of the two diastereomers, as determined by NMR spectroscopy of samples dissolved and analyzed at low temperature. However, dissolution of the crystals in CH_2Cl_2 at room temperature led to the rapid establishment of the ratios of diastereomers observed in the solutions prior to recrystallization (70:30 for **3a** and 43:57 for **3b**). In both cases, the major diastereomer present at equilibrium is the isomer that was isolated by crystallization. The isomerization was sufficiently slow at −78 °C to obtain NMR spectra of the single isomers. Thus, solutions of complexes **3a** and **3b** prepared at −78 °C containing predominantly one isomer were characterized by ^1H NMR, ^{31}P NMR, and 2D-gCOSY-NMR spectroscopies at low temperature. The ^{31}P NMR spectrum at −60 °C of the isolated isomer of the cinnamyliridium complex **3a** consisted of one

DOI: 10.1021/jacs.5b08911
J. Am. Chem. Soc. 2015, 137, 14968−14981

resonance at 97.3 ppm. The ^{1}H and 2D-gCOSY NMR spectrum of the isolated isomer of **3a** contained resonances for the allyl group at 4.90, 4.63, 4.34, and 3.98 ppm. A solution of complex **3b** containing predominantly one isomer generated by dissolving the isolated sample of **3b** in CD_2Cl_2 at −78 °C was also characterized by ^{31}P NMR, ^{1}H NMR spectroscopies. The ^{31}P NMR spectrum consisted of a single peak at 99.7 ppm at −30 °C. The allyliridium complexes **3a** and **3b** also were characterized by high resolution ESI-MS. M^+ values of **3a** and **3b** obtained by ESI-MS matched the calculated values.

The solid-state structure of the major diastereomer of **3a** is shown in Figure 1. The complex adopts a structure that is close to

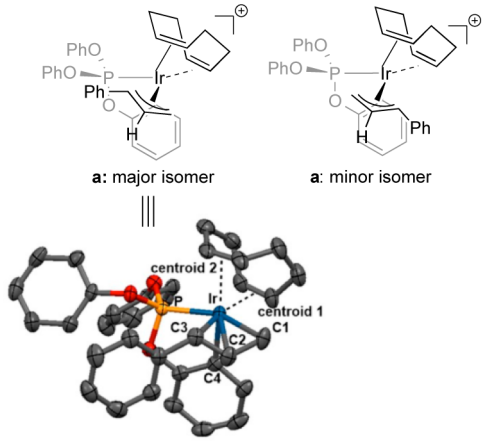

distances (Å)		angles (deg)			
Ir–P	2.256	P–Ir–C3	92.2	cent2–Ir–C1	94.1
Ir–C1	2.285	P–Ir–cent1	104.1	cent2–Ir–cent1	77.7
Ir–C2	2.220	cent1–Ir–C1	99.1	C4–Ir–P	78.0
Ir–C3	2.281	C1–Ir–C3	65.5	C4–Ir–cent1	90.3
Ir–C4	2.092	cent2–Ir–P	97.7	C4–Ir–C1	93.3
Ir–cent1	2.239	cent2–Ir–C3	91.5	C4–Ir–C3	97.3
Ir–cent2	2.356				

Figure 1. ORTEP diagram of **3a** (counterion and hydrogens are omitted for clarity; ellipsoids are drawn to 35% probability).

a six-coordinate octrahedral geometry with the allyl group, phosphorus atom, and an olefin coordinated in one plane. The covalently bound carbon atom and one of the π-bound olefins occupy the two additional, mutually trans positions of the structure.

The relative lengths of the Ir—C_1 and Ir—C_3 bonds have been proposed to influence the regioselectivity of allylic substitution. In complex **3a**, these bond lengths are both 2.28 Å. The similarity between these bond lengths likely results from the binding of the unsubstituted allylic terminus trans to the phosphorus atom and binding of the substituted allylic terminus trans to the equatorial olefin. The stronger trans influence of the phosphine would lengthen the Ir—C bond trans to the phosphorus and the substituent on the other allyl terminus would lengthen the Ir—C bond trans to the olefin. Apparently, the influence of the trans ligand on the Ir—C distance is similar to the influence of the phenyl substituent on the iridium−carbon length.

The ethylene-ligated iridium(I) complex **5** forms by the displacement of the olefinic unit of the allylic substitution product generated by nucleophilic attack on the allyliridium complex **3b**. This complex was characterized by ^{1}H, ^{31}P, and ^{13}C NMR spectroscopies. The ^{31}P NMR spectrum of ethylene-ligated Ir(I) complex **5** in THF consists of a singlet at 128.4 ppm.

Table 1. Reactions of Allyliridium Complexes with Nucleophiles[a]

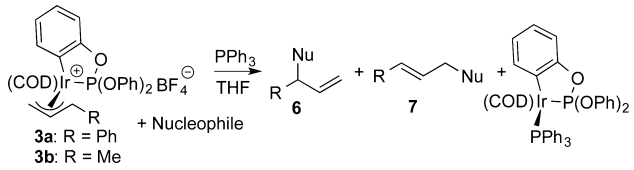

	allyliridium complex	nucleophile	solvent	6:7	yield (%)
1	**3a**	$NaCH(COOMe)_2$	THF	99:1	100
2	**3a**	$NaCMe(COOMe)_2$	THF	97:3	96
3	**3a**	$NaCH(COOMe)_2$	EtOH	95:5	70
4	**3a**	KOPh	THF	94:6	100
5	**3a**	$OctylNH_2$	THF	97:3	100
6	**3a**	$OctylNH_2$	EtOH	99:1	100
7	**3a**	$PhNH_2$/TEA	THF	97:3	60
8	**3b**	$NaCH(COOMe)_2$	THF	99:1	80
9	**3b**	$NaCMe(COOMe)_2$	THF	99:1	96
10	**3b**	KOPh	THF	99:1	70
11	**3b**	$OctylNH_2$	THF	99:1	70

[a]The yields of organic products from the reactions of crotyliridium complex **3b** with sodium malonate, potassium phenoxide, and octylamine were slightly lower than those of the reactions of cinnamyliridium complex **3a** with the same nucleophiles (Table 1, entries 8, 10 and 11). However, the selectivities for the formation of branched organic products were universally high (**6**:**7** = 99:1). The yields of the reactions of crotyliridium complex **3b** with stabilized carbon nucleophiles were similar to the yields of the reactions of cinnamyliridium complex **3a** with the same nucleophiles (Table 1, entries 6 and 7).

Stoichiometric Reactions of Allyliridium Complexes with Nucleophiles and Reactions Catalyzed by Cyclometalated Allyliridium Triphenylphosphite Complexes. Cyclometalated allyliridium triphenylphosphite complexes have been proposed as intermediates in allylic substitution reactions catalyzed by iridium triphenylphosphite complexes.[22] Although cyclometalated iridium triphenylphosphite complexes have been isolated previously,[41−43] they have not been evaluated as potential intermediates in iridium catalyzed allylic substitution reactions. We performed a series of catalytic and stoichiometric reactions to assess the competence of allyliridium complexes **3a** and **3b** to be intermediates in iridium catalyzed allylic substitution reactions.

Stoichiometric Reactions of Allyliridium Complexes 3a and 3b with Nucleophiles. Allyliridium complexes **3a** and **3b** were allowed to react with stabilized enolate, alkoxide, and amine nucleophiles to assess the competence of **3a** and **3b** to be intermediates in iridium catalyzed allylic substitution reactions catalyzed by complexes of iridium containing cyclometalated triphenylphosphite ligands. Suspensions of allyliridium complexes **3a** or **3b** in THF-d_8 were allowed to react with the nucleophiles. These reactions form adducts between the iridium(I) fragment and the alkene unit of the substitution product, as described for addition of aniline and propylamine previously.[16] A slight excess of triphenylphosphine was added to the reaction solutions after full conversion to form the known PPh_3-ligated Ir(I) product and the free organic product.[2] The yield of the reaction was determined by ^{1}H NMR spectroscopy by integrating the peak corresponding to the product vs the internal standard (Si_2Me_6 or mesitylene). The outcome of these stoichiometric reactions is summarized in Table 1.

DOI: 10.1021/jacs.5b08911
J. Am. Chem. Soc. 2015, 137, 14968−14981

The yields of the reactions of cinnamyliridium complex **3a** depended on the strength of the nucleophile. Anionic nucleophiles (Table 1, entries 1, 2, 4) or alkylamine nucleophiles (Table 1, entry 5) formed the products of nucleophilic attack in quantitative yields. However, the reaction of aniline with triethylamine as proton acceptor (Table 1, entry 7) gave a lower yield of the organic product (60%). In this reaction, a small amount of product from double allylation of aniline also formed. Very high regioselectivities for the formation of the branched products were observed for all of the reactions (**6**:**7** > 94:6). Both secondary and tertiary, stabilized carbon nucleophiles formed the branched products with high yield and selectivity (Table 1, entries 1 and 2). Because Takeuchi reported allylic substitutions in ethanol solvent in some cases, we compared the selectivity and yield in EtOH to those in THF. The reactions of octylamine and malonate nucleophiles in EtOH (entries 3 and 6) occurred to give the products in yields and selectivities that are similar to those in THF.

Allylic Substitution Reactions Catalyzed by Allyliridium Complex 3a. The activity of the cyclometalated allyliridium complex **3a** as a catalyst for allylic substitution reactions was assessed with a series of nucleophiles. Ethyl cinnamyl carbonate **1** was allowed to react with stabilized carbon and heteroatom nucleophiles in the presence of 8% cinnamyliridium complex **3a** in THF at 23 °C and EtOH at 50 °C (Table 2, entry 1–2).

Table 2. Allylic Substitution Reactions Catalyzed by Cinnamyliridium Complex 3

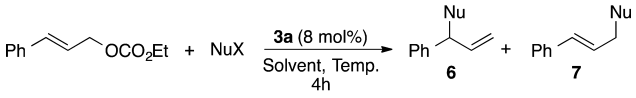

NuX	Solvent	Temp	Yield	6:7
$NaCH(CO_2Me)_2$	THF	25 °C	85%	95:5
octylamine	EtOH	50 °C	87%	>99:1

The reaction of sodium dimethylmalonate with allylic electrophile **1** in THF catalyzed by **3a** formed the allylic substitution product in yields and selectivities that are comparable to those observed for the reactions catalyzed by a mixture of $[Ir(COD)Cl]_2$ and triphenylphosphite in the same medium.[21] The reaction of alkylamines with cinnamyl carbonates catalyzed by $[Ir(COD)Cl]_2$ and $P(OPh)_3$ is reported to occur in refluxing ethanol,[19] and the reaction of octylamine with carbonate **1** catalyzed by isolated **3a** occurred in good yield with high branched-to-linear selectivity in this medium.[44] Moreover, monitoring of the reaction of octylamine with ethyl cinnamyl carbonate catalyzed by the combination of $[Ir(COD)Cl]_2$ and $P(OPh)_3$ in a 1:1 or 1:2 ratio in EtOH by ^{31}P NMR spectroscopy showed that a cyclometalated complex is the catalyst resting state. A single complex was observed by ^{31}P NMR spectroscopy, and this complex was identified by independent synthesis[45] to be the cyclometalated Ir(I) bisposphite complex shown in Figure 2.[46] The formation of this complex from a 1:1 or 1:2 ratio of metal to ligand indicates that the five-coordinate structure with an iridium–carbon bond is more stable than the analogous square-planar complex lacking the κ^1-phosphite; the same type of structure was observed to form with a 1:1 or 1:2 ratio of $[Ir(COD)Cl]_2$ and phosphoramidite ligand previously.[2]

These stoichiometric and catalytic reactions showed that the allyliridium complexes with cyclometalated triphenylphosphite ligand **3a** and **3b** are chemically and kinetically competent to be

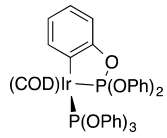

Figure 2. Identity of the resting state of the catalyst in reactions conducted the combination of excess $P(OPh)_3$, $[Ir(COD)Cl]_2$ in EtOH, as determined by ^{31}P NMR spectroscopy.

intermediates in allylic substitution reactions catalyzed by iridium triphenylphosphite complexes. Moreover, these data, in combination with the structural data in Figure 1, speak to the potential origins of regioselectivity proposed for allylic substitution reactions. In the solid-state structure (Figure 1), the substituted allylic terminus is located trans to an olefin, and the unsubstituted terminus is located trans to a phosphorus ligand. The iridium–carbon distance for both allylic termini is the same 2.28 Å. Thus, the observed high selectivity for nucleophilic attack to form the branched allylic substitution product shows that neither the iridium–carbon bond length nor the presence of a soft phosphorus atom trans to the allyl terminus are responsible for the high selectivity of nucleophilic attack at the more substituted position.

Kinetic Studies on Oxidative Addition of Branched and Linear Allylic Acetates to Ethylene-Ligated Iridium(I) Complex 5 Containing a Cyclometalated Triphenylphosphite Ligand. The selectivity for nucleophilic attack at the more substituted position of the allyl group was sufficiently high to prevent a direct assessment of the relative rate for nucleophilic attack at the substituted allylic terminus (to form the branched product) and the unsubstituted allylic terminus (to form the linear product) of allyliridium complexes; the amounts of linear product were too small to measure precisely. However, insight into the relative rates for nucleophilic attack can be gained by studying the kinetics of oxidative addition of branched and linear allylic electrophiles to the cyclometalated Ir(I) triphenylphosphite complex **5**. Studies on the oxidative addition of linear and branched allylic electrophiles can address this issue because this reaction is the reverse of the formal reductive elimination by nucleophilic attack on the allyl complex, and the rates can be measured with these two reactants independently.

The oxidative addition of allylic esters to Ir(I) systems is not strongly favored thermodynamically.[16] Thus, we studied the oxidative addition of allylic trifluoroacetates, which contain a good leaving group and were shown to add to Ir(I) complexes of a cyclometalated phosphoramidite.[18] In particular, the reactions of the linear and branched isomers of the phenalkyl-substituted allylic trifluoroacetates **8** and **9** with the Ir(I) ethylene adduct **5** were studied. These reactions occurred to form an equilibrium mixture of unreacted **5** and two diastereoisomers of allyliridium complexes **3c**.

Due to the reversibility of the reaction, we measured the rate constants for the approach to equilibrium. These measurements were conducted with excess amounts of allylic electrophiles (25 equiv) **8** and **9** and with an excess of ethylene (20 equiv) to render the reaction pseudo-first order in the concentration of ethylene-ligated Ir(I) complex **5**.

The oxidative additions of linear and branched allylic trifluoroacetates **8** and **9** to **5** form allyliridium complex **3c-TFA** as a mixture of two isomers, as determined by ^{31}P NMR spectroscopy (eq 1). These isomers formed in a 65:35 ratio, as determined from the intensities of the ^{31}P NMR signals at 100.2 and 98.6 ppm corresponding to the two complexes. The reaction

DOI: 10.1021/jacs.5b08911
J. Am. Chem. Soc. 2015, 137, 14968–14981

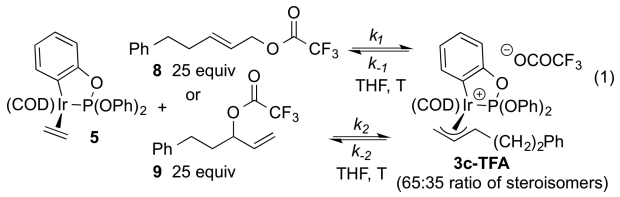

was monitored by ^{31}P NMR spectroscopy, and a plot of concentration vs time for the reaction of branched allylic electrophile **9** with ethylene-ligated complex **5** is provided in Figure 3. The rate constants for oxidative addition were derived

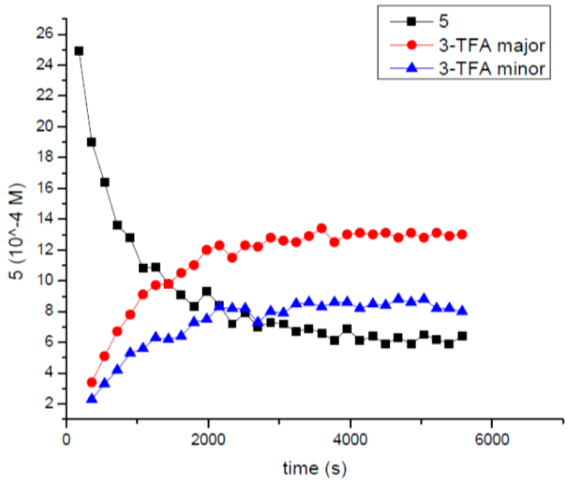

Figure 3. Change of concentration over time graph for the reaction of branched allylic electrophile **9** with ethylene-ligated complex **5**.

from the rate constant of approach to equilibrium and equilibrium constant of the reaction. The rate constants for oxidative addition of linear and branched allylic electrophiles are provided in Table 3, and details of calculation of rate constants are provided in the Supporting Information.

Table 3. Rate Constants for Oxidative Addition of Linear and Branched Allylic Electrophiles 8 and 9 with the Ethylene Ligated Ir(I) Complex 5 (eq 1)

	8 or 9	T (°C)	k_1 or k_2 (s^-)
1	9	−10	8×10^{-4}
2	9	−15	3.5×10^{-4}
3	9	−20	1.3×10^{-4}
4	9	−25	7.5×10^{-5}
5	8	20	2.7×10^{-4}

The rate constants k_1 for the oxidative addition of branched electrophile **9** to ethylene-ligated complex **5** were measured at −10, −15, −20, and −25 °C. The rate constant k_2 for oxidative addition of linear electrophile **8** was measured at 20 °C. To make a direct comparison between the rate constant k_1 and k_2 for addition of the linear and branched allylic esters, respectively, at the same temperature, we extrapolated the rate constants for oxidative addition of branched electrophile **9** to ethylene-ligated complex **5** at the lower temperatures to a rate constant at 20 °C. Activation parameters were derived from an Eyring plot for the rate constants k_2 at −10 to −25 °C (Figure 4). The enthalpy of activation for the reaction of branched electrophile **9** with ethylene ligated complex **5** was 20.5 kcal/mol, and the entropy of

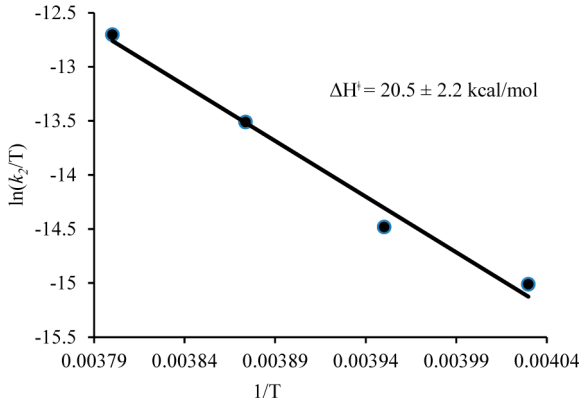

Figure 4. Eyring plot for the oxidative addition of the branched electrophile 9 to ethylene-ligated complex 5.

activation for the same reaction involving dissociation of ethylene and addition of the allylic ester was 4.4 eu. The rate constant for oxidative addition of **9** to **5** at 20 °C was calculated to be 0.046 s^{-1} from these activation parameters.

These kinetic studies showed that the rate constant for oxidative addition of the branched electrophile **9** to ethylene-ligated complex **5** is approximately 170 times faster than the rate constant of oxidative addition of the linear electrophile **8** to Ir(I) complex **5**. This ratio of 170 corresponds to a difference in the free energy of activation of 3.0 kcal. This selectivity is consistent with the observed selectivity for nucleophilic attack to form the branched substitution product over attack to form the linear product.

The difference of 3.0 kcal/mol between the activation energies for oxidative addition of linear and branched electrophiles likely arises from the combination of two factors. The first factor is the difference between the ground state energies of linear allylic trifluoroacetate **8** and branched allylic trifluoroacetate **9**. When an excess of linear allylic trifluoroacetate **8** is allowed to equilibrate in the presence of ethylene ligated complex **5** and excess ethylene, a 3:1 mixture of linear **8** and branched **9** forms. This equilibrium ratio shows that the ground state of linear **8** is 0.64 kcal/mol more stable than the ground state of branched **9**. A second factor that could influence the difference between the two activation energies is the binding energies of the branched and linear alkenes to the cyclometalated iridium center. The branched alkene is a monosubstituted alkene and should have a greater bonding affinity than the linear disubstituted alkene.[47] The contributions from the difference in ground state energies of the allylic esters and the difference in bonding affinity of the two olefins are summarized in Figure 5.

The products from substitution at the least hindered allylic terminus are typically formed by palladium catalysts.[48,49] The difference in selectivity between the palladium-catalyzed allylic substitution and iridium-catalyzed allylic substitution could stem from a smaller difference in bonding affinities of terminal and internal olefins for palladium because the palladium center contains fewer ligands and would be less sterically crowded. However, as will be discussed in detail later in this paper, this difference in affinities of the terminal and internal alkenes to iridium is computed to be similar to the difference in affinities of these alkenes to palladium. Thus, the difference in energy of the terminal and internal alkene complexes could contribute to the formation of branched over linear substitution products but this difference in energy does not distinguish between the selectivity of iridium and palladium complexes. In addition, nucleophilic

DOI: 10.1021/jacs.5b08911
J. Am. Chem. Soc. 2015, 137, 14968−14981

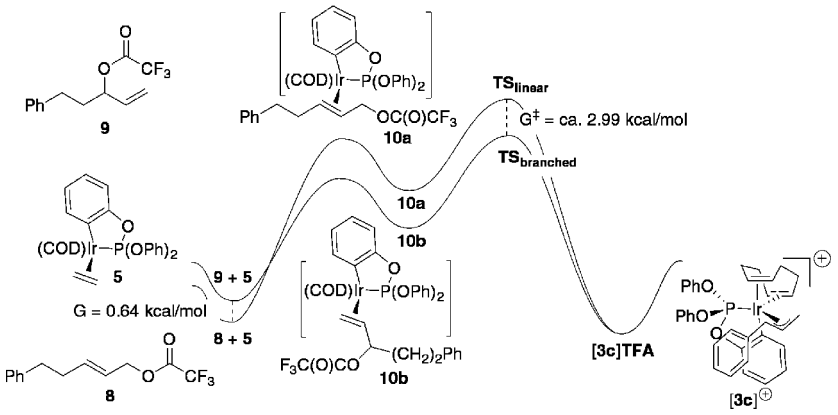

Figure 5. Energy diagram for the reaction of linear and branched allylic electrophiles **8** and **9** with ethylene-ligated complex **5**.

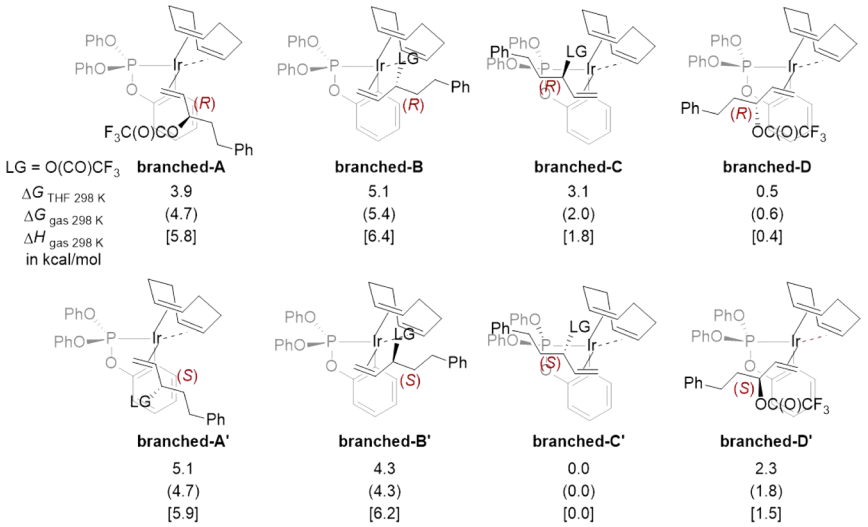

Figure 6. Intermediates of the terminal alkene coordinated iridium complexes.

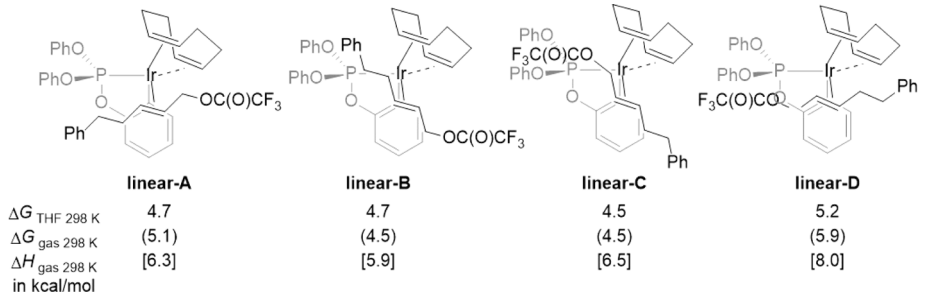

Figure 7. Intermediates of the internal alkene coordinated iridium complexes.

attack by amine nucleophiles on allylpalladium complexes is usually reversible, and this reversibility allows for the formation of thermodynamically more stable linear products and masks the kinetic selectivity for formation of branched products.[38,50]

Computational Study of the Regioselectivity. We conducted DFT calculations to provide additional insight into the origin of the regioselectivity of the iridium catalyzed allylic substitution. We computed the energies of the allyl-iridium complexes that would react with nucleophiles and the energies of the alkene complexes that would precede the oxidative addition to form the allyliridium species. We also computed the activation energies for reactions to form and to consume these complexes. We did so for the complexes with the coordination sphere of the active catalyst containing the unsymmetrical environment created by the cyclometalation process. In addition, we computed these energies for a prototypical palladium complex to assess the origin of the difference in regioselectivity between iridium-catalyzed and palladium-catalyzed allylic substitution. The calculations of the iridium and palladium systems were conducted on reactions involving the formation or cleavage of C—O bonds and C—C bonds to determine the effect of the leaving group and nucleophile on the energetics to form and cleave bonds at the more and less substituted termini of the allyl group.

To begin this portion of our studies, we computed the energies of eight different stereoisomers of the cyclometalated iridium

DOI: 10.1021/jacs.5b08911
J. Am. Chem. Soc. 2015, 137, 14968−14981

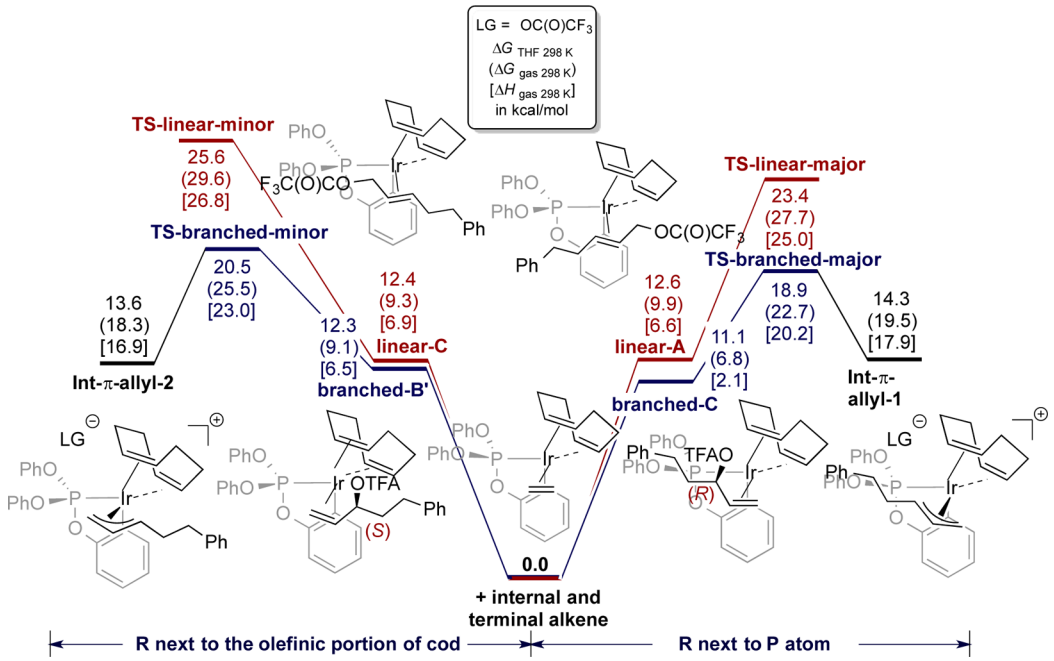

Figure 8. Intermediates and transition states for the oxidative addition of a linear and branched allylic trifluoroacetate to the iridium catalyst.

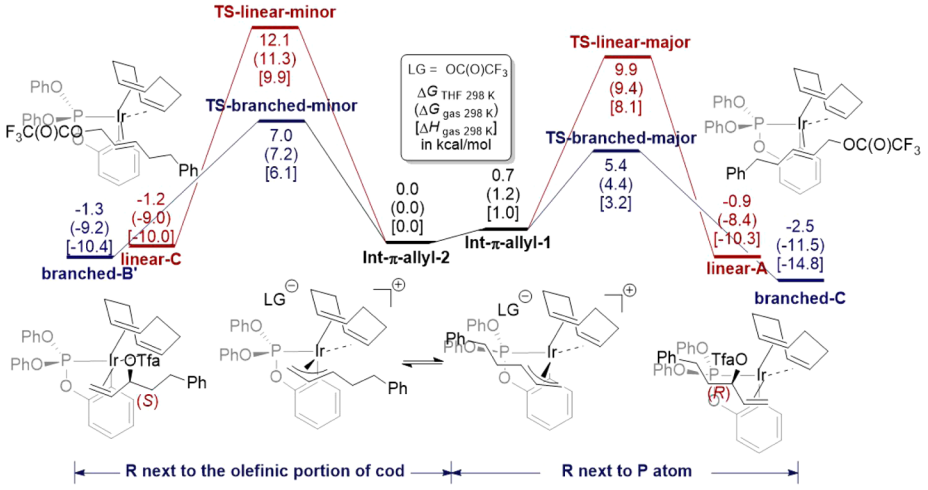

Figure 9. Reductive elimination by nucleophilic attack of trifluoroacetate on the allyliridium catalyst in which the allyl is substituted by a CH_2CH_2Ph group.

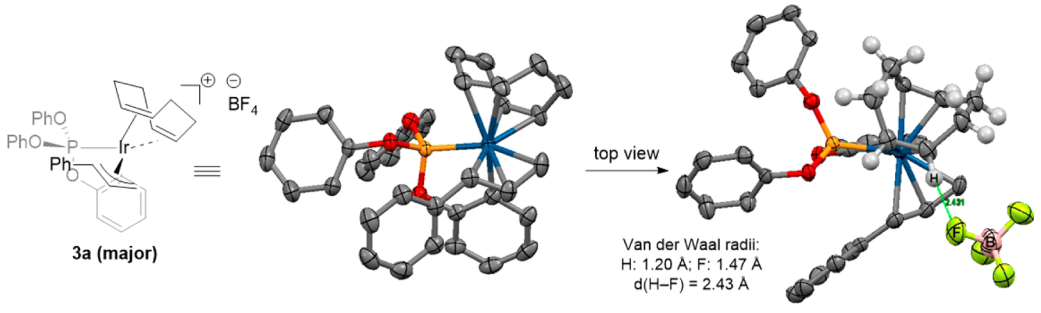

Figure 10. C—H···F attractive interaction in π-allyl complex **3a**.

fragment bound to a terminal alkene (Figure 6). The computed energies of these complexes vary by 5.1 kcal/mol. We also computed the energies of four different stereoisomers of the same metal fragment bound to the *E* internal alkene of the linear allylic trifluoroacetate (Figure 7). The energies of the four stereoisomers of the internal alkene complexes are similar to each other.

We deduced experimentally the structure of the major isomer of the oxidative addition product **3a** (cinnamyl-coordinated iridium complex) by X-ray diffraction (Figure 1). In complex **3a**,

DOI: 10.1021/jacs.5b08911
J. Am. Chem. Soc. 2015, 137, 14968−14981

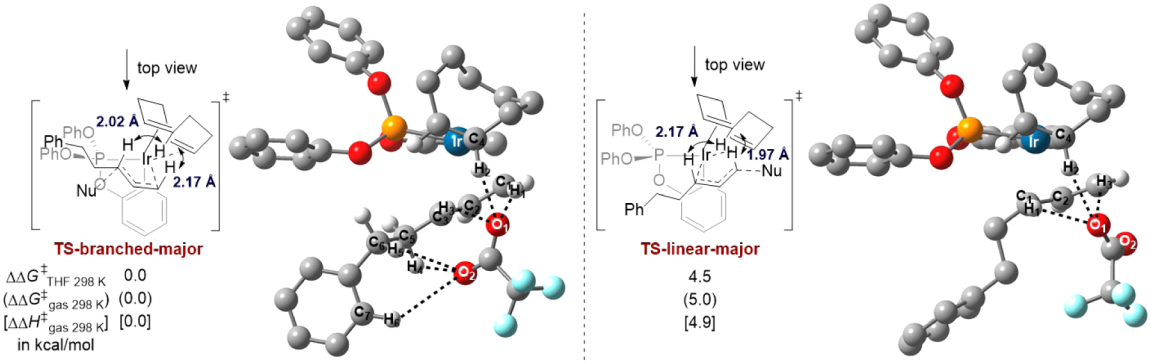

C–H···O interaction	E_{NBO}(C-H activation TS) (in kcal/mol)	d(C–O) (in Å)	d(O–H) (in Å)	∠(C–H–O)
C3–H3···O1	2.25	3.10	2.27	132.4°
C1–H1···O1	1.01	3.25	2.37	137.3°
C4–H2···O1	9.44	3.12	2.05	167.9°
C5–H4···O2	0.23	2.94	2.64	94.9 °
C6–H5···O2	0.90	3.24	2.57	118.4°

C–H···O interaction	E_{NBO}(C-H activation TS) (in kcal/mol)	d(C–O) (in Å)	d(O–H) (in Å)	∠(C–H–O)
C4–H2···O1	4.81	3.27	2.23	159.9°
C1–H1···O1	0.15	3.38	2.61	127.7°
C3–H3···O1	4.49	2.91	2.13	128.7°

difference in C–H···O interaction: branched-linear = 4.4 kcal/mol. $\Delta\Delta G^{\ddagger}_{THF\ 298\ K}$(branched-linear) = 4.5 kcal/mol.

Figure 11. C—H···O interactions in the transition states TS-branched-major and TS-linear-major.

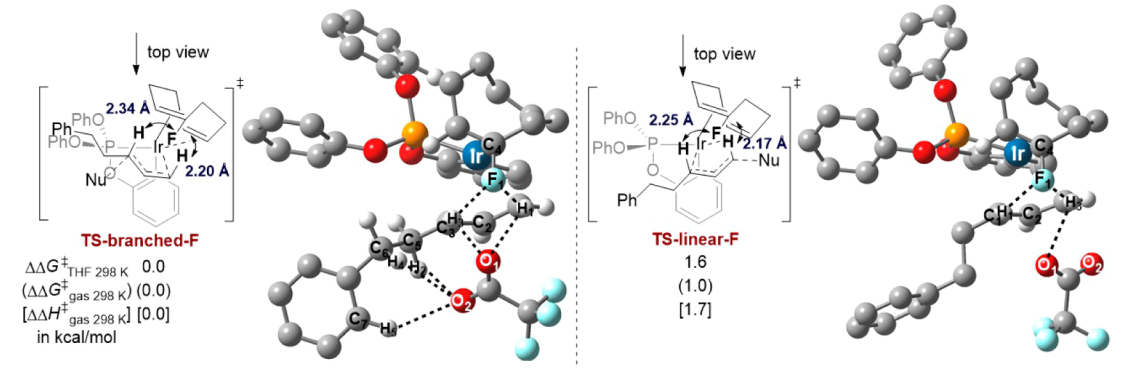

C–H···O interaction	E_{NBO}(C-H activation TS) (in kcal/mol)	d(C–O) (in Å)	d(O–H) (in Å)	∠(C–H–O)
C3–H3···O1	2.53	3.03	2.29	123.4°
C1–H1···O1	0.12	3.43	2.71	123.5°
C5–H2···O2	0.69	2.93	2.47	104.2°
C6–H4···O2	0.45	3.26	2.66	113.8°
C7–H5···O2	0.95	3.61	2.69	142.7°
C3–H3···F1	1.24	3.22	2.35	136.3°
C1–H1···F1	1.78	3.01	2.20	129.6°

C–H···O interaction	E_{NBO}(C-H activation TS) (in kcal/mol)	d(C–O) (in Å)	d(O–H) (in Å)	∠(C–H–O)
C1–H1···O1	0.78	3.00	2.47	108.5°
C3–H3···O1	0.40	3.13	2.63	107.7°
C1–H1···F1	2.30	3.11	2.25	134.9°
C3–H3···F1	2.53	3.01	2.17	132.6°

difference in C–H···O interaction: branched-linear = 1.8 kcal/mol. $\Delta\Delta G^{\ddagger}_{THF\ 298\ K}$(branched-linear) = 1.6 kcal/mol.

Figure 12. C—H···O and C—H···F interactions in the transition states TS-branched-F and TS-linear-F.

the phenyl-substituted terminus of the π-allyl moiety is cis to the phosphorus atom and is trans to the olefinic unit of the cod ligand. In the structure of the related iridium complex (also deduced by X-ray diffraction) generated from a phosphoramide ligand,[17,18] the substituted terminus of the π-allyl moiety is cis to the olefin unit of the cod ligand and is trans to the phosphorus atom. On the basis of these structures, we propose the structure of the minor isomer of the allyliridium complex in the current work to be **3a′** shown in Figure 1. We presume that the alkene complexes, which generate the π-allyl-Ir complex, have the same orientation of the alkyl groups as in the products of the oxidative addition **3a** and **3a′**. Thus, we located the transition states for the oxidative addition from **branched-C**, **linear A**, **branched-B′**, and **linear-C**. These transition states lead to the π-allyl-Ir complexes **Int-π-allyl-1** and **Int-π-allyl-2**, which have the same orientation of the allyl moiety as in complexes **3a** and **3a′**.

As shown in Figure 8, the computed transition states for the reactions of **branched-C** (via **TS-branched-major**) and **branched-B′** (via **TS-branched-minor**) are 18.9 and 20.5 kcal/mol in activation free energy above the combination of the ethylene-ligated iridium catalyst and the free alkenes. In contrast, the computed transition states **TS-linear-major** and **TS-linear-minor** involving oxidative addition of the linear allylic ester **linear-A** and **linear-C** lie 23.4 and 25.6 kcal/mol higher in activation free energy than the combination of uncoordinated alkene and ethylene-coordinated Ir-catalyst. These data indicate that the iridium complexes containing the terminal alkene are much more reactive than the iridium complexes containing the

DOI: 10.1021/jacs.5b08911
J. Am. Chem. Soc. 2015, 137, 14968−14981

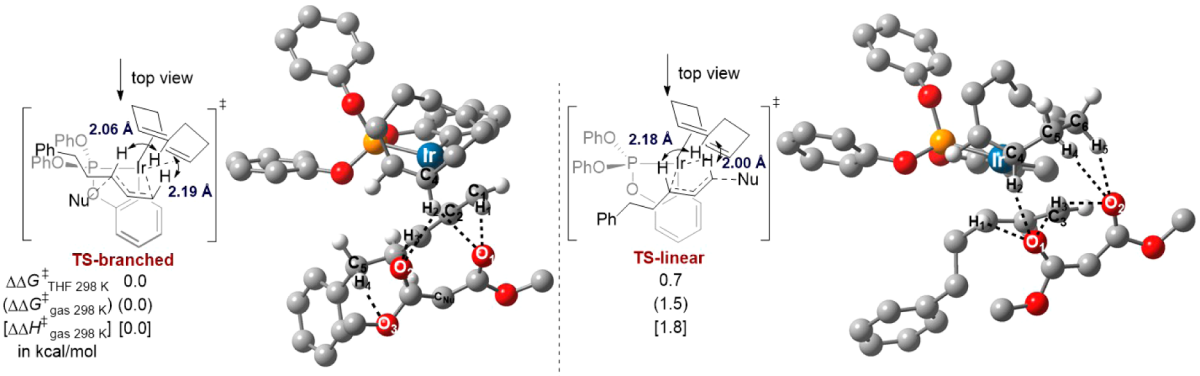

C–H···O interaction	E_{NBO}(C-H activation TS) (in kcal/mol)	d(C–O) (in Å)	d(O–H) (in Å)	∠(C–H–O)
C_1–H_1···O_1	5.97	3.08	2.13	145.5°
C_4–H_2···O_1	1.99	3.44	2.51	143.2°
C_4–H_2···O_2	2.34	3.37	2.45	141.4°
C_3–H_3···O_2	1.50	3.22	2.22	151.6°
C_5–H_4···O_3	0.87	3.50	2.47	156.6°

C–H···O interaction	E_{NBO}(C-H activation TS) (in kcal/mol)	d(C–O) (in Å)	d(O–H) (in Å)	∠(C–H–O)
C_3–H_3···O_1	1.47	3.10	2.33	127.4°
C_1–H_1···O_1	0.11	3.56	2.77	129.6°
C_4–H_2···O_1	3.63	3.27	2.22	160.6°
C_3–H_3···O_2	1.71	3.02	2.30	122.4°
C_5–H_4···O_2	1.58	3.29	2.47	131.6°
C_6–H_5···O_2	0.28	3.42	2.62	129.9°

difference in C–H···O interaction: branched-linear = 3.9 kcal/mol. $\Delta\Delta G^{\ddagger}_{THF\ 298\ K}$(linear-branched) = 0.7 kcal/mol.

Figure 13. C—H···O interactions in transition states involving dimethylmalonate as the nucleophile.

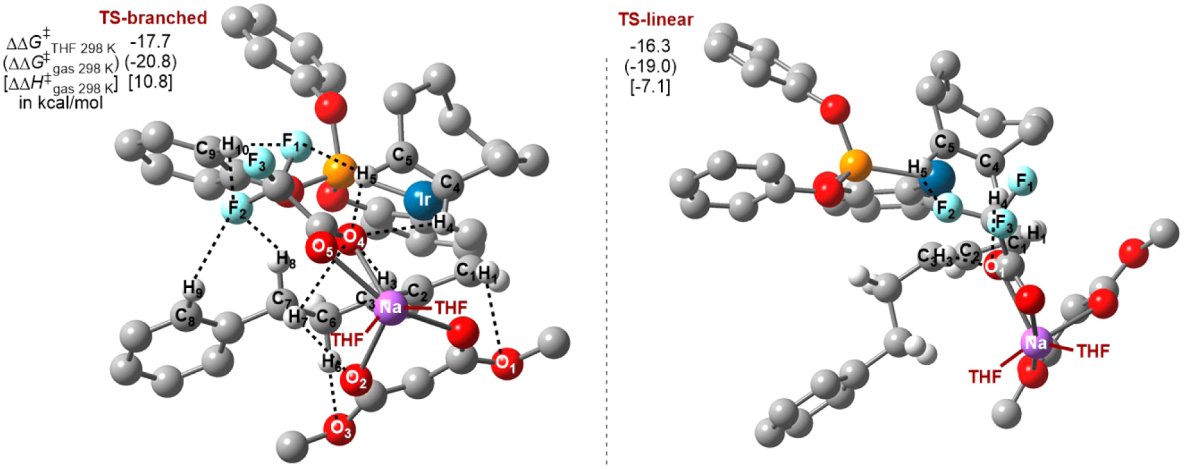

C–H···O interaction	E_{NBO}(C-H activation TS) (in kcal/mol)	d(C–O) (in Å)	d(O–H) (in Å)	∠(C–H–O)
C_1–H1···O_1	0.22	3.26	2.60	118.4°
C_3–H_3···O_4	2.27	3.30	2.32	148.2°
C_4–H_4···O_4	0.21	3.31	2.70	115.3°
C_5–H_5···O_4	2.94	3.13	2.30	131.5 °
C_6–H_6···O_3	1.49	3.30	2.46	132.0°
C_7–H_7···O_2	0.40	3.67	2.68	148.8°
C_7–H_7···O_4	0.17	3.26	2.72	109.7°
C_5–H_5···F_1	1.24	3.26	2.43	132.0°
C_9–H_{10}···F_1	0.87	3.67	2.60	168.2°
C_7–H_8···F_2	0.23	3.51	2.77	125.2°
C_8–H_9···F_2	0.97	3.45	2.49	147.0°
C_9–H_{10}···F_2	0.38	3.47	2.67	130.9°

C–H···O interaction	E_{NBO}(C-H activation TS) (in kcal/mol)	d(C–O) (in Å)	d(O–H) (in Å)	∠(C–H–O)
C_3–H_3···O_1	3.56	3.21	2.17	158.0°
C_4–H_4···O_1	6.39	3.17	2.10	166.3°
C_5–H_5···F_2	0.40	3.41	2.67	124.9°

difference in C–H···O interaction: branched-linear = 1.0 kcal/mol. $\Delta\Delta G^{\ddagger}_{THF\ 298\ K}$(linear-branched) = 1.4 kcal/mol.

Figure 14. C—H···O interactions in transition states involving dimethylmalonate as the nucleophile with NaOTFA as a bridge between the malonate and the iridium complex. The energies are referenced to that for TS-branched in Figure 13.

internal alkene. This finding is consistent with the experimental observation that the rate for oxidative addition of the branched allylic ester containing a terminal alkene is much faster than that of the linear allylic ester containing an internal alkene.

The principle of microscopic reversibility leads to information on the reductive elimination by nucleophilic attack of a trifluoroacetate nucleophile on the π-allyl iridium complex. On the basis of the energetics calculated for oxidative addition,

DOI: 10.1021/jacs.5b08911
J. Am. Chem. Soc. 2015, 137, 14968–14981

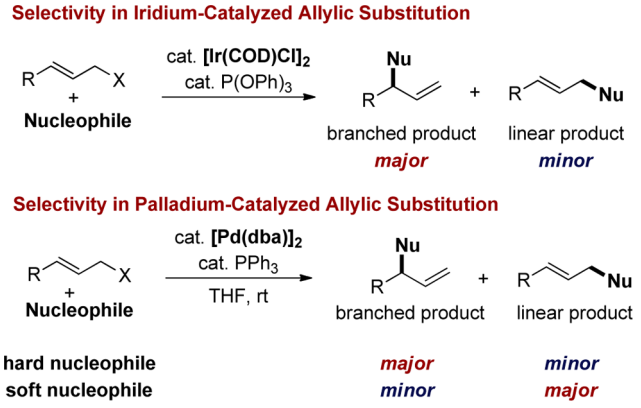

Figure 15. Selectivity in Ir-catalyzed and Pd-catalyzed allylic substitution.

reductive elimination from iridium complex **Int-π-allyl-1** (or **Int-π-allyl-2**) via **TS-branched-major** (or **TS-branched-minor**) to form the branched isomer should be much faster than reductive elimination via **TS-linear-major** (or **TS-linear-minor**) to form the linear isomer of the substitution product (Figure 9). Thus, the energies that we computed by DFT methods are consistent with the experimental observation.

Origin of Regio-Selectivity of the Ir-Catalyzed Allylation. We sought to use these computations to reveal the factors creating the high selectivity of the iridium catalyst for the formation of branched allylic substitution products. Many allyl complexes containing two different donors trans to the allyl ligand have been studied, and the trans effect of these ligands has been proposed to control the regioselectivity with palladium catalysts.[26,28−31] From the above computational data, we could conclude that the ligand located trans to a terminus of the allyl unit does not strongly influence the regioselectivity observed for the reactions catalyzed by the cyclometalated iridium complex. Although the orientation of the allylic termini relative to the phosphite and olefin ligands are different in **TS-branched-major** and **TS-branched-minor** (major and minor refer to the major and minor diastereomers), these two transition states lie at similar free energies. The same result is also observed for the two transition states **TS-linear-major** and **TS-linear-minor** that form the two complexes of the linear allylic substitution products. Because the transition state energies for reaction of the major and minor π-allyliridium complexes are similar to each other, we focused on the reaction pathway for formation of the major diastereoisomer to conserve computational resources.

In the experimental structure of the major diastereoisomer of the π-allyl complex **3a** in Figure 10 determined by single-crystal X-ray diffraction, one of the hydrogen atoms in the cod moiety is close to one of the fluorine atoms in the tetrafluoroborate anion. The distance between these two atoms is only 2.43 Å, which is much shorter than the sum of the Van der Waal radii of hydrogen and fluorine atoms (2.67 Å). This short distance suggests the presence of a C—H···F attractive interaction between the cod ligand and the tetrafluoroborate anion in this π-allyl iridium complex. For our computations on the allylic substitution reaction, we used trifluoroacetate as the nucleophile. Like BF_4^-, trifluoroacetate is anionic; therefore, it could interact with the cod ligand in a similar fashion to BF_4^-. We considered that an attractive C—H···O interaction between the same hydrogen atom in the cod ligand and one of the oxygen atoms in the trifluoroacetate anion could stabilize this structure. The differences in the C—H···O attractive interactions in the transition states to form the branched and linear products might contribute to the regioselectivity of the Ir-catalyzed allylic substitution reactions. With this hypothesis in mind, we analyzed the differences in the computed transition states for the formation of the branched and the linear products.

In these transition states, the two oxygen atoms in the trifluoroacetate nucleophiles are both close to the same C—H bond in the cod ligand (Figure 11). Several additional pairs of C—H···O interactions between the C—H bond in the cod ligand or the C—H bond in the π-allyl moiety and the oxygen atoms in the trifluoroacetate anion appear to be present in this structure. The distances between the hydrogen and oxygen atoms listed in Figure 11 are all shorter than the sum of their van der Waals radii (2.72 Å). These C—H···O interactions appear to serve as bridges between the trifluoroacetate nucleophile and the allyliridium complex, facilitating approach of the nucleophile to the allyl electrophile.

Using NBO second-order perturbation analysis, we computed the stabilization energy provided by these C—H···O interactions in the transition states for attack on the allyliridium species. The C—H···O interactions in the transition state for the formation of the branched product (**TS-branched-major**) are 4.4 kcal/mol stronger than those in the transition state for the formation of the linear product (**TS-linear-minor**). This 4.4 kcal/mol difference in the stabilization energies from the C—H···O interactions in the two transition states is similar to the 4.5 kcal/mol difference in free energies of the same transition states. As a result, we propose that the C—H···O interactions in the transition states for oxidative addition are a major factor contributing to the formation of the branched product for the iridium-catalyzed allylic substitution reaction.

To assess further the effect of the C—H···O interactions on regioselectivity, we computed the structure and reaction of the analogous complexes containing a C—F bond in place of the C—H bond of the cod ligand that we propose participates in C—H···O interactions (Figure 12). In the transition state for reaction of the fluoro−COD complex, one of the strongest C—H···O interactions is absent, and two pairs of C—H···F interactions are now present. The transition state leading to the branched product from the fluoro−COD complex is more favorable than the transition state leading to the linear product, but by only 1.6 kcal/mol. Using NBO second-order perturbation analysis, we obtained the stabilization energy provided by the C—H···O and C—H···F interactions in the nucleophilic substitution transition states. The C—H···O and C—H···F interactions in the transition state forming the branched product (**TS-branched-F**) are 1.8 kcal/mol stronger than those in the transition state leading to the linear product (**TS-linear-F**). The difference in energies of the C—H···X interactions is, again, similar to the difference in energies of the transition states. The smaller difference in transition state energies for the system lacking the strongest C—H···O interaction between the C—H bond in the cod ligand and the oxygen atom in the trifluoroacetate anion is consistent with the importance of this interaction in controlling the relative energies of the transition states. The remaining weak interactions also favor the formation of the branched product, suggesting the importance of a series of weak interactions in controlling the selectivity of these reactions.

In addition to computing the Ir-catalyzed allylic substitution reaction with trifluoroacetate as the nucleophile, we computed the reaction with the anion of dimethylmalonate as nucleophile (the branched/linear selectivity was 10:1 when the dimethylmalonate anion was used in the experiment). The computed energies

DOI: 10.1021/jacs.5b08911
J. Am. Chem. Soc. 2015, 137, 14968−14981

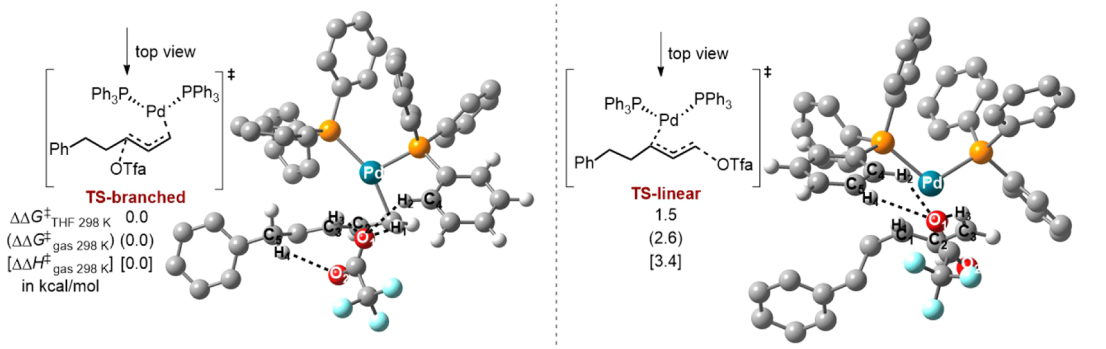

C–H···O interaction	E_{NBO}(C-H activation TS) (in kcal/mol)	d(C–O) (in Å)	d(O–H) (in Å)	∠(C–H–O)
C1–H1···O1	0.33	3.36	2.49	136.5°
C3–H3···O1	4.38	3.02	2.16	134.6°
C4–H2···O1	2.53	3.14	2.24	139.4°
C5–H4···O2	1.30	3.17	2.45	121.9°

C–H···O interaction	E_{NBO}(C-H activation TS) (in kcal/mol)	d(C–O) (in Å)	d(O–H) (in Å)	∠(C–H–O)
C3–H3···O1	5.07	2.95	2.10	132.9°
C4–H2···O1	1.41	3.17	2.38	128.1°
C5–H4···O1	0.25	3.38	2.85	110.2°

difference in C–H···O interaction: branched-linear = 1.8 kcal/mol. $\Delta\Delta G^{\ddagger}_{THF\ 298\ K}$(linear-branched) = 1.5 kcal/mol.

Figure 16. C—H···O interactions in transition states involving trifluoroacetate as the nucleophile in Pd-catalyzed allylation.

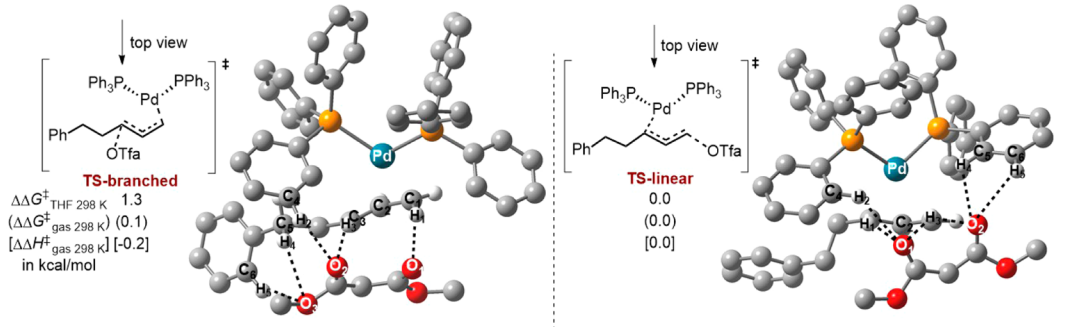

C–H···O interaction	E_{NBO}(C-H activation TS) (in kcal/mol)	d(C–O) (in Å)	d(O–H) (in Å)	∠(C–H–O)
C1–H1···O1	1.03	3.15	2.23	140.5°
C3–H3···O2	0.75	3.30	2.38	142.4°
C4–H2···O2	0.53	3.36	2.67	120.4°
C5–H4···O3	0.30	3.55	2.66	137.9°
C6–H5···O3	0.61	3.73	2.77	147.2°

C–H···O interaction	E_{NBO}(C-H activation TS) (in kcal/mol)	d(C–O) (in Å)	d(O–H) (in Å)	∠(C–H–O)
C3–H3···O1	1.34	3.16	2.35	130.5°
C1–H1···O1	0.38	3.38	2.47	140.0°
C4–H2···O1	0.62	3.51	2.63	137.9°
C3–H3···O2	1.20	3.10	2.36	124.5°
C5–H4···O2	0.29	3.24	2.62	115.0°
C6–H5···O2	0.58	3.25	2.65	114.4°

difference in C–H···O interaction: branched-linear = -1.2 kcal/mol. $\Delta\Delta G^{\ddagger}_{THF\ 298\ K}$(linear-branched) = -1.3 kcal/mol.

Figure 17. C—H···O interactions in transition states involving dimethylmalonate as the nucleophile in Pd-catalyzed allylation.

of the two transition states for addition of dimethylmalonate to form the branched and linear products were closer than those for addition of trifluoroacetate. The computed transition state for the formation of the branched products is only 0.7 kcal/mol lower than that for the formation of the linear product. It is clear from the computational work that the difference in energy is much smaller for the reaction of the more delocalized and more hindered carbon nucleophile, and this result is in accord with the experimental data. However, the NBO second-order perturbation analysis shows that the difference in the stabilization energies contributed by the C—H···O interactions in the transition state is much larger than 0.7 kcal/mol (Figure 13). The difference in the sum of the interaction energies is 3.9 kcal/mol, favoring the formation of the branched product.

We considered that the difference between the energetics of the transition states and the sum of the computed weak interactions could stem from the absence of the cation in our calculations for the addition of the malonate anion. In the experimental system, the electrophile is allyl trifluoroacetate, and the nucleophile is sodium dimethylmalonate. One byproduct is sodium trifluoroacetate, and the sodium trifluoroacetate could function as a bridge between the allyliridum moiety and the dimethylmalonate anion during the nucleophilic substitution. Thus, we computed the transition states containing sodium trifluoroacetate as a bridge, and these structures are shown in Figure 14. Two tetrahydrofuran molecules were used as ligands for sodium to fill two of the six coordination sites around the sodium cation. The other four coordination sites were occupied by the trifluoroacetate and the malonate. The computed transition state for the formation of the branched products was 1.4 kcal/mol lower than that for the formation of the linear product. This value fits the experimentally observed regioselectivity more closely than the value computed in the absence of the sodium trifluoroacetate. Moreover, the stabilization energies contributed by the C—H···O interactions in the transition state were computed by NBO second-order perturbation analysis to be 1.3 kcal/mol in favor of formation of the branched product. This value matches closely with the calculated difference in activation free energy.

DOI: 10.1021/jacs.5b08911
J. Am. Chem. Soc. 2015, 137, 14968−14981

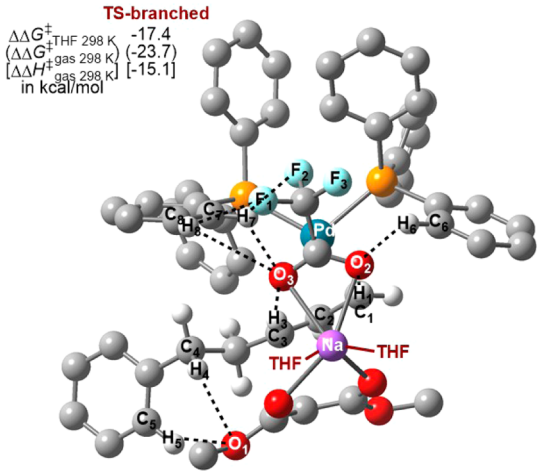

C–H···O interaction	E_{NBO}(C-H activation TS) (in kcal/mol)	d(C–O) (in Å)	d(O–H) (in Å)	∠(C–H–O)
C1–H1···O2	0.37	3.87	2.81	166.5°
C6–H6···O2	1.48	3.48	2.51	147.6°
C3–H3···O3	1.91	3.43	2.37	164.4°
C4–H4···O1	0.62	3.37	2.50	136.2°
C5–H5···O1	0.87	3.55	2.62	142.2°
C7–H7···O3	0.16	3.40	2.66	124.8°
C8–H8···O3	0.10	3.57	3.02	111.4°
C8–H8···F1	0.35	3.65	2.77	138.1°
C7–H7···F2	0.78	3.34	2.50	133.5°

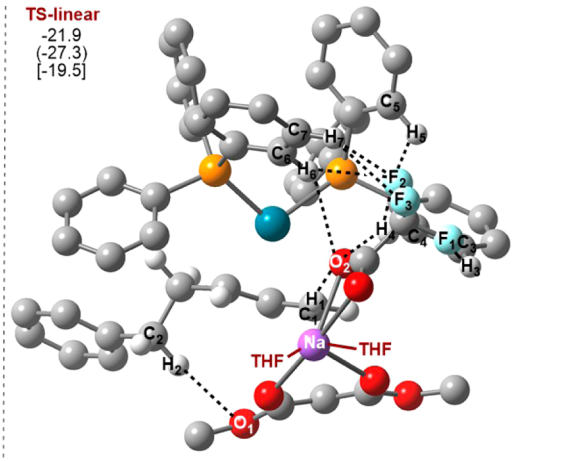

C–H···O interaction	E_{NBO}(C-H activation TS) (in kcal/mol)	d(C–O) (in Å)	d(O–H) (in Å)	∠(C–H–O)
C1–H1···O2	2.58	3.30	2.31	151.9°
C4–H4···O2	4.41	3.32	2.26	163.7°
C3–H3···O3	0.35	3.52	2.77	126.7°
C2–H2···O1	0.11	3.76	2.97	128.8°
C3–H3···F1	0.47	3.42	2.65	127.9°
C4–H4···F2	0.39	3.21	2.55	118.7°
C5–H5···F2	0.23	3.31	2.69	115.7°
C6–H6···F2	0.29	3.32	2.66	118.9°
C7–H7···F2	0.61	3.25	2.50	125.4°
C7–H7···F3	0.26	3.71	2.75	148.3°

difference in C–H···O interaction: branched-linear = -3.3 kcal/mol. $\Delta\Delta G^{\ddagger}_{THF\ 298\ K}$(linear-branched) = -4.5 kcal/mol.

Figure 18. C—H···O interactions in transition states involving dimethylmalonate as the nucleophile with NaOTFA as a bridge between the malonate nucleophile and the palladium catalyst. The energies are referenced to the combination of TS linear in Figure 17 and NaOTFA.

Computational Studies of Analogous Pd-Catalyzed Allylation. It is well established for palladium-catalyzed allylic substitution that reactions of soft nucleophiles, such as malonates and amines, tend to form higher ratios of linear to branched products than do reactions of hard nucleophiles and that they form smaller amounts of the branched products than do reactions catalyzed by complexes of iridium (Figure 15).[23,51,52] To compare the origin of the regioselectivity for reactions of the iridium system to the origin of the regioselectivity for reactions of palladium complexes, we computed the relative energies of the transition states for the formation of linear and branched products from attack of hard and soft nucleophiles on the allylpalladium complex and interactions between the nucleophiles and the allylpalladium species that could control regioselectivity.

We computed the reaction of allylpalladium complexes ligated by PPh_3 with trifluoroacetate and the anion of dimethyl malonate. The allyl group studied contains one phenethyl substituent to match the allyl group on the iridium system we computed. According to our DFT calculations, the reaction of this allylpalladium complex with trifluoroacetate (Figure 16) forms a higher ratio of branched over linear product than does the reaction of the same complex with dimethylmalonate (Figure 17). These computational results are in accord with the experimentally observed selectivity.[27,53]

NBO second-order perturbation analysis was used to reveal the weak interactions that are present in the transition states to form the branched and linear products. This analysis indicates that the stabilization energies contributed by the C—H···O interactions in the transition state to form the branched product from reaction of trifluoroacetate are larger than those in the transition state to form the linear product by 1.8 kcal/mol. In contrast, the stabilization energies contributed by the C—H···O interactions in the transition state for nucleophilic attack by dimethylmalonate are larger in the transition state to form the linear product than they are in the transition state to form the branched product by 1.2 kcal/mol.

Because the reaction of the anion of a malonate with an allylic ester would contain an alkali metal counterion and the reaction would contain alkali metal carboxylate as a byproduct, we also computed activation free energies for reaction of dimethylmalonate with the allylpalladium species in the presence of sodium trifluoroacetate as a bridge between the allyl moiety and the dimethylmalonate anion (Figure 18). The activation free energy computed for this reaction is much lower than that computed for this reaction without sodium trifluoroacetate. For the structures that include sodium trifluoroacetate, the difference between the free energies of the transition states for formation of the linear and branched products from addition of the anion of dimethyl malonate is 4.5 kcal/mol, favoring the formation of the linear product.[54] This value is also similar to the difference in weak interactions between the two transition states (3.1 kcal/mol favoring the formation of the linear product).

These two examples of the Pd-catalyzed allylic substitution reactions and the NBO second-order perturbation analysis of the structures of the transition states suggest that the C—H···O interactions, again, are a major factor controlling the regioselectivities for the allylic substitution. However, the

DOI: 10.1021/jacs.5b08911
J. Am. Chem. Soc. 2015, 137, 14968−14981

regioselectivity for the reactions of allylpalladium complexes changes when different nucleophiles are used. Unlike the C—H···O interactions in the iridium system, which favor the formation of the branched product for all the nucleophiles studied, the C—H···O interactions in the palladium system are computed to be stronger for formation of the linear product than for formation of the branched product with the soft nucleophile, but are computed to be stronger for formation of the branched product than for formation of the linear product with the hard nucleophile.

CONCLUSIONS

Allyliridium complexes **3a** and **3b** ligated by a cyclometalated triphenylphosphite were prepared. Through a series of stoichiometric and catalytic reactions, these allyliridium complexes were found to be competent intermediates in allylic substitution reactions catalyzed by a combination of iridium and triphenylphosphite. The regioselectivity of stoichiometric and catalytic reactions, along with solid state structural data, showed that iridium−carbon bond lengths or the presence of a *trans*-phosphorus do not influence the position of nucleophilic attack. These conclusions were coorobrated by results of computational studies. Ethylene-ligated Ir(I) complex **5** containing a cyclometalated triphenylphosphite ligand was prepared from allyliridium complexes **3a** and **3b**. Kinetic measurements on oxidative addition of branched and linear allylic electrophiles to ethylene-ligated complex **5** showed that oxidative addition of branched electrophiles is faster than oxidative addition of linear electrophiles. Computational studies on the origin of the regioselectivity of the allylic substitution reactions catalyzed by the iridium-triphenylphosphite system showed that the relative strength of the C—H···O interactions in the transition state for the formation of the branched and linear products appears to be a major factor controlling the regioselectivity. The C—H···O interactions were computed to be stronger in the transition state leading to the branched products from iridium-catalyzed reactions of both heteroatom and carbon nucleophiles. Calculations on the regioselectivity of the reactions of allylpalladium complexes ligated by triphenylphosphine also support the proposal that the difference in the C—H···O interactions in the transition state for nucleophilic attack is a major factor controlling the site of attack.

ASSOCIATED CONTENT

Supporting Information

The Supporting Information is available free of charge on the ACS Publications website at DOI: 10.1021/jacs.5b08911.

Experimental methods, characterization of complexes and reaction products, and supplementary kinetic data (PDF)
Computational output (CIF)

AUTHOR INFORMATION

Corresponding Author

*jhartwig@berkeley.edu

Notes

The authors declare no competing financial interest.

ACKNOWLEDGMENTS

This work was supported by NIGMS in the National Institutes of Health (GM-55382). We thank Johnson−Matthey for a gift of $[Ir(COD)Cl]_2$. We thank Dr. Konstantin Troshin for obtaining NMR spectra of the products of catalytic reactions.

REFERENCES

(1) Ohmura, T.; Hartwig, J. F. *J. Am. Chem. Soc.* **2002**, *124*, 15164.
(2) Kiener, C. A.; Shu, C.; Incarvito, C.; Hartwig, J. F. *J. Am. Chem. Soc.* **2003**, *125*, 14272.
(3) Hartwig, J. F.; Stanley, L. M. *Acc. Chem. Res.* **2010**, *43*, 1461.
(4) Hartwig, J. F.; Pouy, M. J. *Top. Organomet. Chem.* **2011**, *34*, 169.
(5) Alexakis, A.; Polet, D. *Org. Lett.* **2004**, *6*, 3529.
(6) Tissot-Croset, K.; Polet, D.; Alexakis, A. *Angew. Chem., Int. Ed.* **2004**, *43*, 2426.
(7) Helmchen, G.; Dahnz, A.; Dubon, P.; Schelwies, M.; Weihofen, R. *Chem. Commun.* **2007**, 675.
(8) Lyothier, I.; Defieber, C.; Carreira, E. M. *Angew. Chem., Int. Ed.* **2006**, *45*, 6204.
(9) Singh, O. V.; Han, H. *J. Am. Chem. Soc.* **2007**, *129*, 774.
(10) Singh, O. V.; Han, H. *Org. Lett.* **2007**, *9*, 4801.
(11) Zhuo, C.-X.; Zheng, C.; You, S.-L. *Acc. Chem. Res.* **2014**, *47*, 2558.
(12) Liu, W.-B.; Xia, J.-B.; You, S.-L. *Top. Organomet. Chem.* **2011**, *38*, 155.
(13) Liu, W.-B.; Reeves, C. M.; Stoltz, B. M. *J. Am. Chem. Soc.* **2013**, *135*, 17298.
(14) Tosatti, P.; Nelson, A.; Marsden, S. P. *Org. Biomol. Chem.* **2012**, *10*, 3147.
(15) Kiener, C. A.; Shu, C. T.; Incarvito, C.; Hartwig, J. F. *J. Am. Chem. Soc.* **2003**, *125*, 14272.
(16) Markovic, D.; Hartwig, J. F. *J. Am. Chem. Soc.* **2007**, *129*, 11680.
(17) Madrahimov, S. T.; Markovic, D.; Hartwig, J. F. *J. Am. Chem. Soc.* **2009**, *131*, 7228.
(18) Madrahimov, S. T.; Hartwig, J. F. *J. Am. Chem. Soc.* **2012**, *134*, 8136.
(19) Takeuchi, R.; Ue, N.; Tanabe, K.; Yamashita, K.; Shiga, N. *J. Am. Chem. Soc.* **2001**, *123*, 9525.
(20) Takeuchi, R.; Kashio, M. *J. Am. Chem. Soc.* **1998**, *120*, 8647.
(21) Takeuchi, R.; Kashio, M. *Angew. Chem., Int. Ed. Engl.* **1997**, *36*, 263.
(22) Helmchen, G.; Dahnz, A.; Duebon, P.; Schelwies, M.; Weihofen, R. *Chem. Commun.* **2007**, 675.
(23) Poli, G.; Prestat, G.; Liron, F.; Kammerer-Pentier, C. *Top. Organomet. Chem.* **2011**, *38*, 1.
(24) Acemoglu, L.; Williams, J. M. J. *Handbook of Organopalladium Chemistry for Organic Synthesis* **2002**, *2*, 1689.
(25) Trost, B. M.; Toste, F. D. *J. Am. Chem. Soc.* **1999**, *121*, 4545.
(26) Ward, T. R. *Organometallics* **1996**, *15*, 2836.
(27) Åkermark, B.; Hansson, S.; Krakenberger, B.; Vitagliano, A.; Zetterberg, K. *Organometallics* **1984**, *3*, 679.
(28) Pretot, R.; Pfaltz, A. *Angew. Chem., Int. Ed.* **1998**, *37*, 323.
(29) Sprinz, J.; Kiefer, M.; Helmchen, G.; Reggelin, M.; Huttner, G.; Walter, O.; Zsolnai, L. *Tetrahedron Lett.* **1994**, *35*, 1523.
(30) Brown, J. M.; Hulmes, D. I.; Guiry, P. J. *Tetrahedron* **1994**, *50*, 4493.
(31) Togni, A.; Burckhardt, U.; Gramlich, V.; Pregosin, P. S.; Salzmann, R. *J. Am. Chem. Soc.* **1996**, *118*, 1031.
(32) Pamies, O.; Dieguez, M.; Claver, C. *J. Am. Chem. Soc.* **2005**, *127*, 3646.
(33) Helmchen, G.; Pfaltz, A. *Acc. Chem. Res.* **2000**, *33*, 336.
(34) Mata, Y.; Pàmies, O.; Diéguez, M. *Adv. Synth. Catal.* **2009**, *351*, 3217.
(35) Leahy, D. K.; Evans, P. A. In *Modern Rhodium-Catalyzed Organic Reactions*; Evans, P. A., Ed.; Wiley-VCH: Weinheim, 2005; p 191.
(36) Trost, B. M.; Lautens, M. *J. Am. Chem. Soc.* **1983**, *105*, 3343.
(37) Trost, B. M.; Lautens, M. *Tetrahedron* **1987**, *43*, 4817.
(38) Watson, I. D. G.; Yudin, A. K. *J. Am. Chem. Soc.* **2005**, *127*, 17516.
(39) Dubovyk, I.; Watson, I. D. G.; Yudin, A. K. *J. Am. Chem. Soc.* **2007**, *129*, 14172.
(40) Spiess, S.; Raskatov, J.; Gnamm, C.; Brödner, K.; Helmchen, G. *Chem. - Eur. J.* **2009**, *15*, 11087.
(41) Bedford, R. B.; Castillòn, S.; Chaloner, P. A.; Claver, C.; Fernandez, E.; Hitchcock, P. B.; Ruiz, A. *Organometallics* **1996**, *15*, 3990.

DOI: 10.1021/jacs.5b08911
J. Am. Chem. Soc. 2015, 137, 14968−14981

(42) Lin, C.-H.; Lin, C.-Y.; Hung, J.-Y.; Chang, Y.-Y.; Chi, Y.; Chung, M.-W.; Chang, Y.-C.; Liu, C.; Pan, H.-A.; Lee, G.-H.; Chou, P.-T. *Inorg. Chem.* **2012**, *51*, 1785.
(43) Lin, C.-H.; Chang, Y.-Y.; Hung, J.-Y.; Lin, C.-Y.; Chi, Y.; Chung, M.-W.; Lin, C.-L.; Chou, P.-T.; Lee, G.-H.; Chang, C.-H.; Lin, W.-C. *Angew. Chem., Int. Ed.* **2011**, *50*, 3182.
(44) The reaction with octylamine in THF did not provide detectable amounts of allylic substitution products. Considering both oxidative addition of allyl carbonate and nucleophilic addition to allylic complex **1** occurs at room temperature in THF, we speculate that this lack in reactivity in THF is due to competing or irreversible binding of amine to the iridium (I) complex.
(45) Bedford, R. B.; Castillón, S.; Chaloner, P. A.; Claver, C.; Fernández, E.; Hitchock, P. B.; Ruiz, A. *Organometallics* **1996**, *15*, 3990.
(46) The balance of the iridium in reactions with a 1:1 ratio of iridium to ligand is, presumably, unreacted $[Ir(COD)Cl]_2$.
(47) Hartley, F. R. *Chem. Rev.* **1973**, *73*, 163.
(48) Hayashi, T.; Konishi, M.; Kumada, M. *J. Chem. Soc., Chem. Commun.* **1984**, 107.
(49) Hayashi, T.; Yamamoto, A.; Hagihara, T. *J. Org. Chem.* **1986**, *51*, 723.
(50) Mackenzie, P. B.; Whelan, J.; Bosnich, B. *J. Am. Chem. Soc.* **1985**, *107*, 2046.
(51) Trost, B. M.; Crawley, M. L. *Chem. Rev.* **2003**, *103*, 2921.
(52) Dubovyk, I.; Watson, I. D. G.; Yudin, A. K. *J. Org. Chem.* **2013**, *78*, 1559.
(53) Åkermark, B.; Zetterberg, K.; Hansson, S.; Krakenberger, B.; Vitagliano, A. *J. Organomet. Chem.* **1987**, *335*, 133.
(54) The difference in free energies of activation for formation of the linear and branched products in the absence of sodium trifluoroacetate (Figure 17) fits the value deduced from the experimental regioselectivity more closely than the value in the absence of sodium trifluoroacteatee. The experimental linear/branched selectivity is between 2:1 and 9:1, depending on the allylic electrophile and the nucleophile. However, the energies of activation in Figure 18 are 17−22 kcal/mol lower than those in Figure 17. Although the difference in selectivity in Figure 18 is slightly larger than that corresponding to the experimental selectivity, the transition states do favor formation of the linear product and the difference in activation energies differ from the experimental values by only about 3 kcal/mol.

DOI: 10.1021/jacs.5b08911
J. Am. Chem. Soc. 2015, 137, 14968−14981